



The synthesis, photochemical and biological properties of new silicon phthalocyanines

Canan Uslan, B. Şebnem Sesalan*

Istanbul Technical University, Faculty of Science and Letters, Department of Chemistry, Maslak 34469, Istanbul, Turkey

ARTICLE INFO

Article history:

Received 5 March 2012

Received in revised form 21 June 2012

Accepted 11 August 2012

Available online 23 August 2012

Keywords:

Silicon phthalocyanine

DNA

Fluorescence

Quaternization

Photocleavage of DNA

ABSTRACT

Bis[(1-methylpyrrolidin-2-yl)methoxy] [phthalocyaninato] silicon (**2**), bis[2-azepan-1-yl]ethoxy] [phthalocyaninato] silicon (**3**) and bis[(2,4,6-tris(*N,N*-dimethylamminomethyl) phenoxy)] [phthalocyaninato] silicon (**4**) were prepared and they were quaternized with the excess of iodomethane to obtain the compounds **2Q**, **3Q** and **4Q** respectively. The binding of quaternized **2Q**, **3Q** and **4Q** phthalocyanines (pcs) with calf thymus (CT) DNA was investigated by UV–Vis, fluorescence spectrophotometric methods and gel electrophoresis. The quenching effect of all quaternized pcs on the fluorescence intensity of SYBR Gold (SYBR)–DNA complex was determined. The results indicated that novel pcs exhibit efficient DNA binding activity. Photocleavage of CT-DNA in the presence of **2Q**, **3Q** and **4Q** were determined using gel electrophoresis. All the experimental data proved that these pcs might be the candidates as DNA-targeting PDT agents.

© 2012 Elsevier B.V. All rights reserved.

1. Introduction

DNA plays an increasingly important role in bioorganic chemistry, biotechnology, and material science. Owing to the central role of DNA in replication and transcription, it has been a major target for antibiotic, anticancer, and antiviral drugs [1]. The effects of nucleic acid binding drugs are known for various diseases such as cancer, malaria, AIDS, and other viral, bacterial, and fungal infections [2]. Since physicochemical properties of phthalocyanines (pcs) can be easily adjusted by modification of the electronic distribution on the aromatic ring through peripheral substitutions, they have been studied as dyes [3], light emitting diodes, in molecular electronics, for non-linear optical applications, as liquid crystals, gas sensors, semiconductor materials, in photovoltaic cells and for electrochromic displays [4–6]. In addition, they can be used in immunohistochemistry, imaging the retinal veins and cardiovascular system as well as photodynamic therapy (PDT) of cancer and photoinactivation of bacteria [7–9]. Pcs have a long-wavelength band with a large extinction coefficient ($\sim 10^5 \text{ M}^{-1} \text{ cm}^{-1}$) and generally a low dark toxicity. Some are efficient $^1\text{O}_2$ generators [6,10–13]. The ability of phthalocyanines to photoinactivate mammalian cells was reported first by Ben-Hur and Rosenthal in 1985 [14].

Of particular interest are positively charged pcs, since such molecules could potentially target highly vulnerable intracellular sites and cause effective DNA photodamage. The central metal ion and

peripheral substituents play an important role in the photophysical properties of pcs. A silicon phthalocyanine (pc), Pc 4, has attracted considerable interest as a PDT agent since it was reported to be used in PDT in 1993 [15–19]. Si(IV)-Pcs containing one or two bulky axial ligands usually show reduced aggregation, enhanced water solubility, and high photodynamic efficacy. Recently, two glucosylated Si(IV)-Pcs were shown to have high phototoxicity toward human carcinoma HT29 and HepG2 cells [10] and a Si(IV)-Pc bearing two solketal axial substituents was found to be highly phototoxic to both 14C and B16F10 cell lines [20].

The interaction of silicon pcs with DNA, photoinactivation of HIV and combination of them with platinum units were reported as efficient DNA-targeted PDT agents [21,22]. The peripheral substituents and axial ligands govern to an important extent the physical, chemical and biological properties of these compounds and make it possible to prepare satisfactorily optimized pcs for use as photosensitizers.

Among the different pcs employed for DNA binding studies, the positively charged pcs are the most efficient ones in terms of binding and cleaving DNA as compared with either the neutral or negatively charged pcs. In this perspective, the main scope of this work is to synthesize new silicon pcs (Fig. 1) which have the potential use for cancer treatment. We work on the synthesis of pcs and porphyrazines with different functional moieties such as heterocyclic groups, porphyrazine–phthalocyanine hybrid units and quaternized amino groups [23–30].

To clarify the binding mode of novel pcs (Fig. 2) to CT-DNA, UV–Vis and fluorescence titration experiments, DNA gel electrophoresis were performed and the changes in CT-DNA thermal

* Corresponding author. Tel.: +90 212 285 33 03; fax: +90 212 285 63 86.

E-mail address: sungurs@itu.edu.tr (B. Şebnem Sesalan).

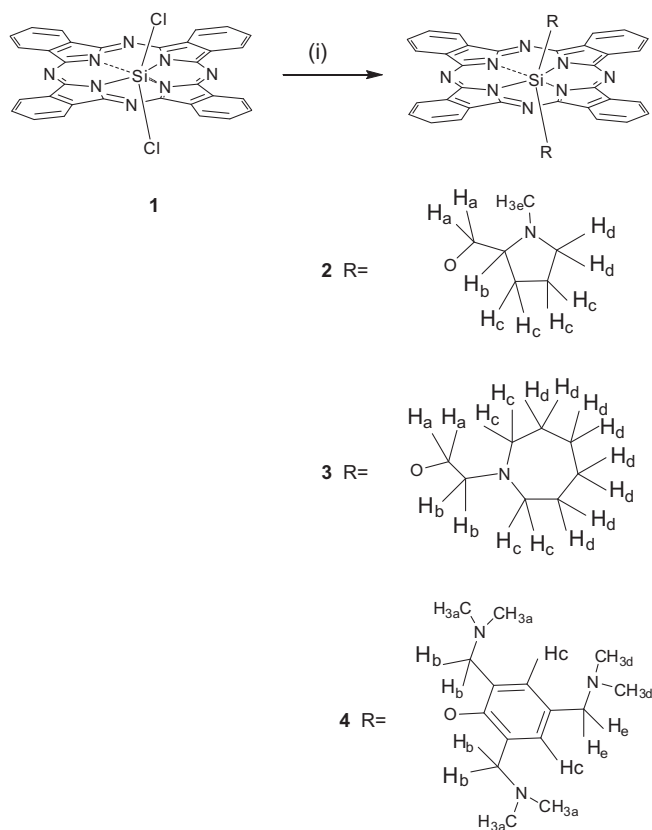


Fig. 1. The synthetic pathway of the compounds **2**, **3** and **4**. (i) Dry toluene, NaH, 6 h, reflux.

denaturation profiles were determined. Furthermore, quenching effect of novel pcs on the fluorescence intensity of SYBR–DNA complex with Stern–Volmer constants were calculated. Afterwards, we studied the photo-induced DNA cleaving abilities of these macrocycles.

2. Experimental

2.1. Materials

All reagents and solvents were of reagent grade quality and were obtained from commercial suppliers. 1-Methylpyrrolidin-2-yl-methanol, 2-azepan-1-yl-ethanol, 2,4,6-tris(*N,N*-dimethylaminomethyl) phenol and dichloro [phthalocyaninato] silicon were purchased from Aldrich. SYBR Gold was purchased from Fluka.

2.2. Equipment

^1H NMR spectra were recorded on a Varian Mercury 200 MHz spectrometer in CDCl_3 and DMSO-d_6 . Chemical shifts were reported (δ) relative to Me_4Si as internal standard.

Positive ion and linear mode MALDI-MS of complexes were obtained in dihydroxybenzoic acid as MALDI matrix using nitrogen laser accumulating 50 laser shots using Bruker Microflex LT MALDI-TOF mass spectrometer.

IR spectra were recorded on a Perkin-Elmer Spectrum One FT-IR spectrophotometer and electronic spectra on Scinso Neosys 2000 double beam UV–Vis Spectrophotometer with 1 cm path length quartz cuvettes in the spectral range of 300–800 nm.

Elemental analyses were performed with Thermo Finnigan Flash EA 1112 at 950–1000 °C.

Melting temperature study was carried out using a thermostated Shimadzu-1901 UV–Vis spectrophotometer.

Fluorescence and UV–Vis spectra were recorded on a Perkin-Elmer LS55 fluorescence and Scinso SD 1000 spectrophotometer, respectively.

2.3. Determination of binding of **2Q**, **3Q** and **4Q** to DNA using UV–Vis titrations

All titrations of pcs with CT-DNA were performed at room temperature in distilled water. The concentrations of CT-DNA per nucleotide phosphate ($[\text{DNA}]$) was calculated from the absorbance at 260 nm using $\epsilon_{\text{DNA}} = 6600 \text{ M}^{-1} \text{ cm}^{-1}$ [31]. DNA was stored at 4 °C overnight and used within 2 days. 0.62 mM DNA, 0.04 mM **2Q**, **3Q** and **4Q** stock solutions were prepared in distilled water. A 1.5 mL aqueous solution of **2Q**, **3Q** or **4Q** was placed in 3 mL quartz cuvette (a final concentration of 3.6 μM) and 10 x 10 μL injections of DNA were added manually. Absorption spectra were collected from 300 to 800 nm. The titrations were carried out until pcs' Q bands remain at a fixed wavelength upon the successive additions of CT-DNA.

2.4. Determination of binding **2Q**, **3Q** and **4Q** to DNA using fluorescence measurements

The binding of water soluble complexes **2Q**, **3Q** and **4Q** to DNA were studied by spectrofluorometry at room temperature. An aqueous solution of **2Q**, **3Q** or **4Q** (1 μM , 2.5 mL) was titrated by successive additions of 5 μL aliquots of 5 μM DNA. After each addition of DNA, the fluorescence emission spectra were recorded. The concentration of DNA along the titration varied from 0 to 0.059 μM . Fluorescence excitation and emission spectra were obtained from solutions of DNA and quaternized pcs (**2Q–4Q**) were prepared in distilled water. Excitation and emission slits were set at 7 nm bandpass at 900 V. Pcs solutions were excited at 610 nm and spectra were recorded between 650 and 750 nm. The steady diminution in pcs fluorescence with increase in DNA concentrations was noted and used in the determination of the binding constants and the number of binding sites on DNA, according to Eq. (3) [32].

$$nQ + B \leftrightarrow Qn + B \quad (1)$$

where B is biomolecule like pc (unbound or free form), Qn is DNA with n binding sites. Here, $Qn + B$ is the quenched biomolecule (pc when bound to DNA) whose association constant is K_a .

$$K_a = [Qn + B] / ([Q]^n [B]) \quad (2)$$

If the overall amount of pcs is B_0 , then $[B_0] = [B] + [Qn + B]$. Here $[B]$ is the concentration of the unbound pc. According to this data, the relationship between the fluorescence and the unbound pc can be defined as $[B]/[B_0] = F/F_0$ where F is the fluorescence of the unbound pc during the addition of DNA and F_0 is the initial intensity of pc

$$\log(F_0 - F)/F = \log K_a + n \log [\text{DNA}] \quad (3)$$

where F_0 and F are the fluorescence intensities of pc complex (**2Q**, **3Q** or **4Q**) in the absence and presence of DNA respectively; K_a , the binding constant; n , the number of binding sites on DNA; and $[\text{DNA}]$ the concentration of DNA solution. Plots of $\log[(F_0 - F)/F]$ against $\log [\text{DNA}]$ would provide the values of n (from the slope) and K_a (from the intercept). The experiments were repeated three times and standard deviations were given in Table 1.

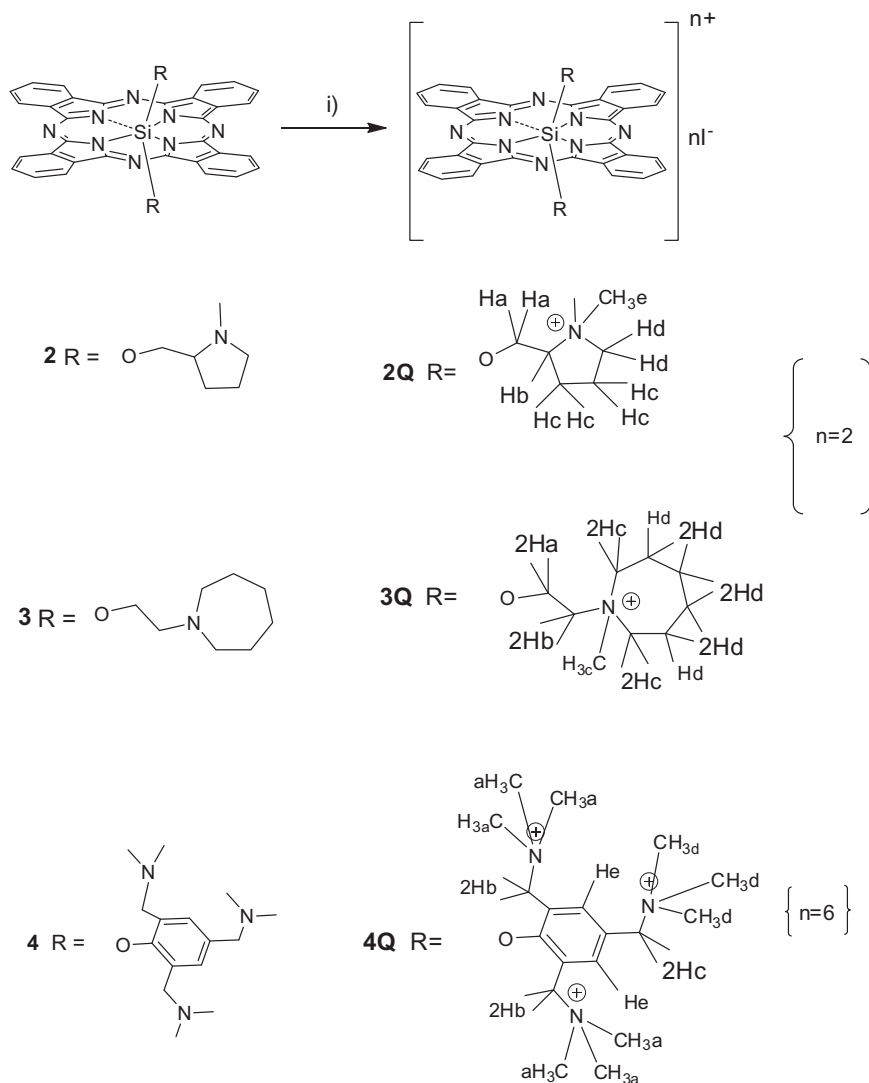


Fig. 2. The synthesis of quaternized phthalocyanines **2Q**, **3Q** and **4Q**. (i) CH_2Cl_2 , CH_3I , 25 °C, 4 h.

Table 1
 K_a , K_{sv} and n values of compounds with standard deviations (\pm STD) **2Q**, **3Q** and **4Q**.

	2Q	3Q	4Q
$K_a (\times 10^3)$ (L/mol)	7.048 ± 0.8	5.370 ± 0.7	2.089 ± 0.8
K_{sv} (L/mol)	1.35 ± 0.7	0.794 ± 0.8	0.473 ± 0.8
n	0.61 ± 0.8	0.52 ± 0.7	0.56 ± 0.8

2.5. Determination of quenching effect of **2Q**, **3Q** and **4Q** on the fluorescence intensity of DNA–SYBR complex by using K_{sv} constants

In order to determine the binding mode of **2Q–4Q** pcs to DNA, the decrease in emission of DNA–SYBR complex around 540 nm was monitored indicating the competitive binding of SYBR with quaternized pcs **2Q–4Q**. The concentration of the purchased SYBR Gold was 10000 \times and was diluted to 1 \times . Each of six fluorescence cuvettes contained the solution of SYBR at a fixed concentration of 1 \times (200 μL) and the solution of DNA (5 μM , 1.8 mL). At a final concentration of 0, 0.1, 0.25, 0.5, 0.75 and 1 μM , 200 μL solutions of quaternized pcs **2Q–4Q** were added to the solution of SYBR–DNA complex in each cuvette. The samples were excited at 497 nm and the spectra were recorded from 520 to 650 nm consecutively

at 900 V with a slit of 7 nm for both excitation and emission. All solutions were prepared in distilled water.

The quenching effect of quaternized pcs **2Q–4Q** on the fluorescence of SYBR–DNA complex was calculated by using Stern–Volmer relationship [33] according to Eq. (4):

$$F_0/F = 1 + K_{sv}[\text{pc}] \quad (4)$$

where F_0 and F are the fluorescence intensities of the excited DNA–SYBR complex in the absence and presence of pcs, $[\text{pc}]$ is the concentration of **2Q**, **3Q** or **4Q** and K_{sv} is the Stern–Volmer constant. The slope of the plots of F_0/F versus $[\text{pc}]$ provide the value of K_{sv} which indicates the affinity of quaternized pcs **2Q–4Q** to DNA. The measurements were repeated three times and standard deviations were calculated.

2.6. Determination of the change in thermal denaturation profile of DNA

Melting temperatures were determined for CT-DNA (0.062 mM, 2.5 mL) and **2Q**, **3Q** or **4Q** (0.021 mM, 0.1 mL) in water by heating from 25 to 90 °C at a rate of 0.6 °C/min, recording the UV absorbance at 260 nm every 10 s.

2.7. Determination of binding **2Q**, **3Q** and **4Q** to DNA using gel electrophoresis

The binding of compounds **2Q–4Q** to DNA was further studied by gel electrophoresis. *R* refers to the ratio of [MPC]/[DNA]. 2.7 µM DNA, 1 µM **2Q**, **3Q** and **4Q** solutions were prepared in distilled water and used in ratio given in Table 1. Staining solution was prepared in Tris/borate/EDTA (TBE). The products were run at 120 V for 20 min 1% agarose gel, stained with SYBR and analyzed photographically under UV light.

2.8. Determination of singlet oxygen generation of **2Q**, **3Q** and **4Q**

Photo-irradiations were done using a 600–700 nm diode laser. A dichroic filter (Schimadzu) was additionally placed in the light path before the sample. A 3 mL portion of the respective substituted pc derivatives; **2Q**, **3Q** and **4Q**, (concentration = 1×10^{-5} M) containing the singlet oxygen quencher was irradiated in the Q band region with the photo-irradiation set-up described in references [34,35]. 9,10-Antracenediyl-bis(methylene)dimalonic acid (ADMA) was used as chemical quencher for singlet oxygen in aqueous media. To avoid chain reactions induced ADMA in the presence of singlet oxygen [36], the concentration of ADMA was lowered to $\sim 3 \times 10^{-5}$ M. Solutions of sensitizer containing ADMA were prepared in the dark and irradiated in the Q band region using the set-up described above. ADMA degradation at 380 nm (in water) was monitored. Spectra were recorded every 5 s.

2.9. Determination of photocleavage of plasmid DNA using gel electrophoresis

The experiments were performed in 0.5 mL plastic eppendorf microcentrifuge tubes. Each tube contained 10 µL (0.2 µg) of supercoiled DNA (pBR322) and 0.87 µM **2Q**, **3Q** and **4Q** solutions were prepared in distilled water. Tubes were illuminated from top and in air at room temperature with 600–700 nm diode laser which was placed 5 cm away from the tested tubes. Irradiation time changed from 1 to 5 s. without changing the concentrations of the reactants in each tube. After irradiation, conversion of supercoiled DNA (form I) to nicked circular DNA (form II) was visualized by 1% agarose gel electrophoresis and subsequent SYBR staining. To test the involvement of singlet oxygen in photocleavage, 0.2 M (5 µL) sodium azide was used.

2.10. Synthesis

2.10.1. The general route for the synthesis of bis[(1-methylpyrrolidin-2-yl)methoxy] [phthalocyaninato] silicon (**2**), bis[2-azepan-1-yl]ethoxy] [phthalocyaninato] silicon (**3**) and bis(2,4,6-tris(*N,N*-dimethylamminomethyl) phenoxy) [phthalocyaninato] silicon (**4**)

A mixture of unsubstituted dichloro [phthalocyaninato] silicon (**1**) (50 mg, 0.0817 mmol), NaH (0.735 mmol, 17.6 mg) and (1-methylpyrrolidin-2-yl)methanol (28.21 mg, 0.245 mmol) for compound **2**, 2-(azepan-1-yl)ethanol (35.08 mg, 0.245 mmol) for compound **3** or 2,4,6-tris(*N,N*-dimethylaminomethyl) phenol (65 mg, 0.245 mmol) for compound **4** in dry toluene (25 mL) was refluxed for 6 h under N_2 . After the reaction mixture was centrifuged, the filtrate was evaporated and the residue was washed with *n*-hexane (3 × 30 mL) and dried *in vacuo*.

Data for compound **2**: The crude product was subjected to aluminum oxide column chromatography and was purified by using dichloromethane/methanol (10/1) as eluent (Fig. 1). Yield: 38 mg (61.2%). IR ν_{\max} (cm^{-1}): 2773; 1611; 1519; 1471; 1426; 1333; 1287; 1163; 1119; 1076; 985; 908; 757. 1H NMR ($CDCl_3$): -2.29 – (-1.85) (d, 4H, Ha); (-0.54) – (-0.77) (m, 2H, Hb); 1.26–1.27 (m, 8H, Hc); 1.62–2.07 (t, 4H, Hd); 2.08–3.20 (s, 4H, He);

8.05–8.07 (m, 8H, H β); 9.33–9.35 (m, 8H, H α). Anal. Calc. for $C_{44}H_{40}N_{10}O_2Si$: C, 69.10; H, 5.54; N, 17.39. Found: C, 68.73; H, 5.24; N, 17.01%.

Data for compound **3**: The crude product was subjected to aluminum oxide column chromatography and was purified by using tetrahydrofuran/chloroform (10/1) as eluent (Fig. 1). Yield: 35 mg (52.2%). IR ν_{\max} (cm^{-1}): 3011; 2907; 1613; 1520; 1426; 1332; 1288; 1164; 1121; 1077; 1050; 1004; 952; 909; 758. 1H NMR (acetone- d_6): -1.92 – (-1.89) (t, 4H, Ha), 0.30–0.34 (t, 4H, Hb); 1.71–1.83 (m, 16H, Hd); 3.45–3.51 (m, 8H, Hc); 8.35–8.42 (m, 8H, H β); 9.58–9.62 (m, 8H, H α). Mass (MALDI-TOFF): *m/z* calculated for $C_{48}H_{48}N_{10}O_2Si$ [M] $^+$: 825.05; found 825.48. Anal. Calc. for $C_{48}H_{48}N_{10}O_2Si$: C, 69.80; H, 6.07; N, 16.90. Found: C, 69.88; H, 5.86; N, 16.98%.

Data for compound **4**: Firstly, the oily residue was reacted with tetrahydrofuran (30 mL) at room temperature 1 h. Then the mixture was centrifuged and the impurities were precipitated and the filtrate was evaporated. Secondly the residue was dissolved in acetone (30 mL) and the impurities were precipitated. The filtrate was evaporated under vacuum until it was dry. The crude product was then washed with cold hexan (2 × 30 mL) and then cold diethyl ether (3 × 30 mL) (Fig. 1). Yield: 31 mg (35.6%). IR ν_{\max} (cm^{-1}): 3011; 2942; 2855; 2815; 2771; 1606; 1357; 1313; 1247; 1173; 1144; 1097; 1025; 986; 880; 836. 1H NMR (DMSO- d_6): 1.17–1.33 (m, 8H, Hb); 2.22–2.03 (m, 24H, Ha); 2.23–2.32 (br s, 12H, Hc); 2.33–2.40 (br s, 4H, Hd); 6.91–6.98 (m, 4H, He); 8.44–8.67 (m, 8H, H β); 9.54–9.77 (m, 8H, H α). Mass (MALDI-TOFF): *m/z* calculated for $C_{62}H_{68}N_{14}O_2Si$ [$M-2$] $^+$: 1067.38; found 1067.48. Anal. Calc. for $C_{62}H_{68}N_{14}O_2Si$: C, 69.60; H, 6.38; N, 18.30. Found: C, 69.63; H, 6.41; N, 18.29%.

2.10.2. The general route for the synthesis of quaternized bis[(1-methylpyrrolidin-2-yl)methoxy] [phthalocyaninato] silicon (**2Q**), bis[2-azepan-1-yl]ethoxy] [phthalocyaninato] silicon (**3Q**) and bis(2,4,6-tris(*N,N*-dimethylamminomethyl) phenoxy) [phthalocyaninato] silicon (**4Q**)

The quaternization of neutral compounds **2**, **3** and **4** was prepared according to the previous work [25]. Briefly, the compound **2**, **3** or **4** (100 mg, 0.13 mmol) was dissolved in CH_2Cl_2 (30 cm^3) and stirred with excess CH_3I (185 mg, 1.56 mmol) at room temperature for 4 h. The mixture was then filtered and the precipitate was washed with CH_2Cl_2 (5 × 30 mL) and dried *in vacuo*.

Data for the compound **2Q**: Yield: 72 mg (52.9%). IR ν_{\max} (cm^{-1}): 2883; 1976; 1610; 1521; 1472; 1429; 1335; 1292; 1166; 1114; 1080; 957; 910; 791; 757. 1H NMR (DMSO- d_6): -2.30 – (-2.22) (d, 4H, Ha); -1.81 – (-1.77) (m, 2H, Hb); 1.65–1.87 (m, 8H, Hc); 2.25–2.33 (m, 4H, Hd); 3.06 (s, 12H, He); 8.28–8.34 (m, 8H, H β); 9.45–9.51 (m, 8H, H α) (Fig. 2). Mass (MALDI-TOFF): *m/z* calculated for $C_{46}H_{46}N_{10}O_2Si^{2+}$ [$M-2I+1$] $^+$: 800.01; found 800.08. Anal. Calc. for $C_{46}H_{46}N_{10}I_2Si$: C, 52.50; H, 4.38; N, 13.28. Found: C, 52.48; H, 4.40; N, 13.30%.

Data for the compound **3Q**: Yield: 62 mg (46.3%). IR ν_{\max} (cm^{-1}): 2851; 2579; 1974; 1610; 1519; 1472; 1428; 1335; 1291; 1162; 1121; 1078; 998; 947; 909; 852; 790; 758; 717. 1H NMR (DMSO- d_6): -2.16 – (-2.05) (t, 4H, Ha); 0.50–0.54 (t, 4H, Hb); 2.23–2.09 (m, 16H, Hd); 2.81–2.90 (m, 14H, Hc); 8.16–8.22 (m, 8H, H β); 9.32–9.34 (m, 8H, H α) (Fig. 2). Mass (MALDI-TOFF): *m/z* calculated for $C_{50}H_{54}N_{10}O_2Si^{2+}$ [$M-2I+1$] $^+$: 856.11; found 856.07. Anal. Calc. for $C_{50}H_{54}N_{10}I_2Si$: C, 54.18; H, 4.89; N, 12.60. Found: C, 54.15; H, 4.91; N, 12.63%.

Data for the compound **4Q**: Yield: 50 mg (27.9%). IR ν_{\max} (cm^{-1}): 3012; 2943; 1608; 1478; 1377; 1337; 1250; 1163; 1124; 1082; 1011; 973; 911; 870; 777. 1H NMR (D_2O): 1.67–1.93 (br s, 8H, Hb); 2.59–2.92 (br s, 36H, Ha); 2.94–2.97 (s, 4H, Hc); 2.98–3.22 (s, 18H, Hd); 7.73–8.00 (m, 4H, He); 8.02–8.69 (s, 8H, H β); 9.23–10.00 (m, 8H, H α) (Fig. 2). Mass (MALDI-TOFF): *m/z* calculated for $C_{65}H_{77}N_{14}O_2Si^{3+}$ [$M-6I-3CH_3$] $^+$: 1114.48; found 1114.21.

Anal. Calc. for $C_{68}H_{86}N_{14}I_6Si$: C, 42.50; H, 4.49; N, 10.18. Found: C, 42.52; H, 4.51; N, 10.21%.

3. Results and discussion

3.1. Synthesis

The synthetic procedures of the pc complexes **2–4** and **2Q–4Q** were given in Figs. 1 and 2. New silicon pcs were prepared in the presence of NaH for deprotonation of alcohol derivatives or phenol. While the compound **1** was insoluble in toluene, the new products **2**, **3** and **4** were soluble. Excess of iodomethane was used in order to obtain complete quaternization. For the characterization of compounds 1H NMR, IR, mass spectra and elemental analysis results were used. All reactions were followed by TLC (thin layer chromatography) and the compounds **2** and **3** were purified with column chromatography. Since the compound **4** was basic due to the amine groups, purification with chromatographic methods (it was adsorbed even on basic alumina) were unsuccessful. However, elemental analysis results of all compounds were in accordance with the calculated ones.

For the compound **2**, vibrations at 1076 cm^{-1} indicated Si–O bond in IR spectrum. Around 1076 cm^{-1} Si–O vibrations were observed in IR spectrum. In 1H NMR spectrum, due to magnetic anisotropy [37], a and b protons were observed between -2.29 – (-1.65) ppm as doublet and (-0.54) – (-0.77) ppm as multiplet, respectively. C protons were seen between 1.26 and 1.27 ppm. The shifts between 1.62–2.07 ppm and 3.20–2.08 ppm were attributed to N–CH₂ (d) protons and N–CH₃ (e) protons respectively. The characteristic α and β protons of pc macrocycle were seen between 9.33–9.35 ppm and 8.05–8.07 ppm, respectively (Fig. 1). Molecular ion peak of **2** was not observed in MALDI-TOFF spectrum. However elemental analysis results were consistent with the calculated ones.

In IR spectrum of **2Q**, vibrations at 1080 cm^{-1} were proved the presence of Si–O bond. In 1H NMR spectrum, e protons which were attributed to hydrogens of methyl groups attached to nitrogen were observed at 3.06 ppm as singlet. A and b protons were observed between -2.30 – (-2.22) ppm and between -1.81 – (-1.77) ppm, respectively. Magnetic anisotropy was effective for a and b protons which were close to Si–O bond indicating the shielding effect of pc macrocycle [37]. The shifts between 1.65–1.87 ppm were attributed to c protons. N–CH₂ (d) protons were observed between 2.25–2.33 ppm. The shifts between 8.28–8.34 ppm and 9.45–9.51 ppm indicated the characteristic β and α protons in pc ring, respectively (Fig. 2). In mass spectrum of compound **2Q** showed the base peak cleavage of anion as is often observed for this type of compounds [38].

For compound **3**, in IR spectrum vibrations 1077 cm^{-1} confirmed Si–O bond. In 1H NMR spectrum proved the presence of shielding effect of pc molecule on a and b protons which were substituted directly on the macrocycle with the shifts observed between -1.92 – (-1.89) ppm and 0.30–0.34 ppm, respectively. D protons were seen as multiplet between 1.71–1.83 ppm. The shifts between 3.45–3.51 ppm were attributed to N–CH₂ (c) protons. α and β protons of pc macrocycle were seen between 9.58–9.62 ppm and 8.35–8.42 ppm, respectively (Fig. 1). Molecular ion peak; $[M]^+$ at 825.48 was observed and supported the expected structure together with elemental analysis results.

IR spectrum of compound **3Q** supported the Si–O bond with the vibrations at 1078 cm^{-1} . Further, 1H NMR spectrum of **3Q** quaternized methyl groups were observed at 2.81–2.90 ppm and d protons between 2.23–2.09 ppm as multiplet. A and b protons were seen between -2.16 – (-2.05) ppm and (-0.54) – (-0.77) ppm respectively. Characteristic β and α protons of pc ring were seen between 8.16–8.22 ppm and 9.32–9.34 ppm respectively (Fig. 2). In mass spectrum

of compound **3Q** showed the base peak cleavage of anion as is often observed for this type of compounds [38]. Cationic molecular ion peak; $[M-21+1]^+$, was seen at 856.07 and was harmonized with calculated value.

For compound **4**, in IR spectrum vibration at 1097 cm^{-1} showed Si–O bond. In 1H NMR spectrum of **4**, shifts between 1.17–1.33 ppm for b protons and 2.22–2.03 ppm for a protons indicated magnetic anisotropy of the pc ring [39]. According to integral areas, *p*-N–CH₃ protons (c) and *p*-N–CH₂ protons (d) were shown between 2.23–2.32 ppm and 2.33–2.40 ppm, respectively. Aromatic protons were seen between 6.91–6.98 ppm. β protons between 8.44–8.67 ppm and α protons were observed between 9.54–9.77 ppm (Fig. 1). In mass spectrum $[M-2]^+$ peak was observed at 1067.48 *m/z*. Elemental analysis results supported the expected structure.

In IR spectrum of **4Q**, vibrations at 3012 cm^{-1} supported the existence of aromatic structure and vibrations at 1082 cm^{-1} indicated the formation of Si–O bond. In 1H NMR spectrum, due to shielding effect of pc ring, the shifts between 2.59–2.92 ppm and 1.67–1.93 ppm were attributed to a and b protons respectively. According to integral areas, c and d protons were seen between 2.94–2.97 ppm and 2.98–3.22 ppm respectively. Aromatic protons (e) protons were shown around 7.73 ppm. β protons between 8.02–8.69 ppm and α protons were observed between 9.23–10.00 ppm (Fig. 2). MALDI-TOFF mass spectrum of **4Q** showed the base peak cleavage of anion and methyl as is often observed for this type of compounds [38].

3.2. Determination of binding of **2Q**, **3Q** and **4Q** to DNA using UV-Vis measurements

While DNA intercalating agents cause large shifts at wavelengths, groove binding or stacking are observed by small changes in absorbances or wavelengths in the UV-Vis spectrum [31].

The more the increase in aggregation, the more the decrease in maximum was observed. Thick black lines in Fig. 3 (lines from 9 to 11 in Fig. 3a and b and lines from 8 to 11 in Fig. 3c were overlapping each other indicated that after addition of 80 μL CT-DNA to **2Q** and **3Q**, 70 μL CT-DNA to **4Q**, the Q band absorbance remained constant) showed the end of titration which means maximum interaction between pcs and DNA occurred. According to Fig. 3a and b **2Q** and **3Q** displayed neither blue nor red shift around Q-band (683 nm for **2Q** and 684 nm for **3Q**) as well as in Soret band region. In case of **2Q** and **3Q**, the lack of shift in band maxima and a small hypochromicity of quaternized pcs was consistent with simple electrostatic binding between positive pc and negative phosphate backbone of DNA and was due to small axial ligands substituted to pc ring inhibiting closer stacking [40]. There was no shift around Q band (688 nm) region in UV-Vis spectrum of **4Q** as well as **2Q** and **3Q** while a red shift from 308 nm to 311 nm indicating an existence of external binding [41] (Fig. 3c). As reported earlier [41], intercalative binding displays a much larger spectral shift as well as hypochromicity in the absorption spectrum than external monomeric binding or outside stacking due to the π - π interaction between pc plane and the DNA base pairs. When we compared the narrow Q band of **2Q** and **3Q** with broad one of **4Q**, aggregation due to amine groups caused a broad and less intense Q band as shown in Fig. 3c. Upon the addition of DNA, the aggregation among bulky quaternized amines in compound **4Q** caused so small decrease in absorbance around Q band region that hypochromicity was nondistinguishable [42]. Since the phthalocyanines are macromolecules, small or planar substituents may result intercalative binding. Here, as proved with K_a values, the smallest cationic group (in **2Q**) has more affinity to interact with DNA more than **3Q** and **4Q** supporting non-intercalative but minor groove binding. Axial groups in silicon phthalocyanines also inhibit aggregation and promote minor

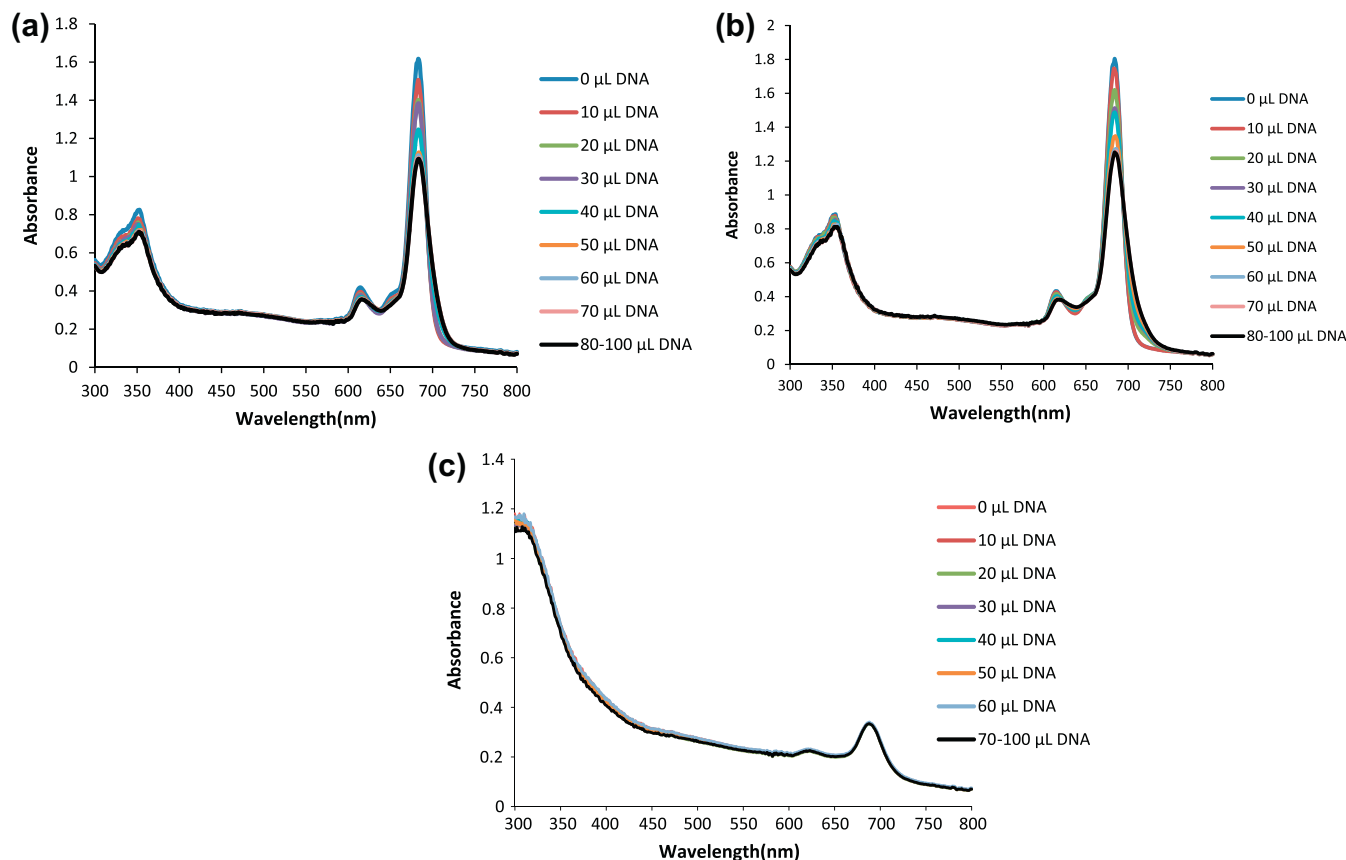


Fig. 3. Electronic spectra of **2Q** (a), **3Q** (b) and **4Q** (c) upon increasing amounts of CT-DNA. 10 successive injections (each contained 10 μL 0.62 mM CT-DNA) were added to 3.6 μM , 1.5 mL aqueous solution of **2Q**, **3Q** or **4Q**. Line 1: spectrum of the solution which contained 3.6 μM , 1.5 mL of **2Q** (a), **3Q** (b) or **4Q** (c). Line 2–8: The decrease in absorbance continued (Line 2 (10 μL) to line 8 (70 μL)) until a stable **2Q** or **3Q**-Pc complex formed. Line 9 (80 μL)-Line 11 (100 μL) (bold black lines): A stable DNA-Pc complex formed when 80 μL , 0.62 mM CT-DNA was added to **2Q** (a) or **3Q** (b) and 70 μL to **4Q** (c).

groove binding but not intercalative binding [43]. These results were in accordance with K_a values: $7.048 \pm 0.8 \times 10^3$ (for **2Q**), $5.370 \pm 0.7 \times 10^3$ (for **3Q**) and $2.089 \pm 0.8 \times 10^3$ (for **4Q**).

3.3. Determination of binding **2Q**, **3Q** and **4Q** to DNA using fluorescence measurements

The data obtained from the titration of the compounds with DNA also allowed calculating the drug/DNA association constants (K_a), according to a previously proposed model [32] (Eq. (3)). The association constants were given in Table 1 and Fig. 4 supporting a non-intercalative but minor groove binding with DNA. Examination of the obtained K_a values allowed interpreting that the addition of small hydrophilic cationic groups in **2Q** and **3Q** increased the affinity of the molecules towards DNA. Van Der Waals interactions and hydrogen bonding are the main forces leading the smaller molecules to the minor groove. Opposite to that, bulky substituents such as phenyl rings in **4Q** hindered the binding process and decreased the affinity to DNA. K_a values were calculated as $0.48 \pm 0.8 \times 10^3$, $5.370 \pm 0.7 \times 10^3$ and $2.089 \pm 0.8 \times 10^3$ for **2Q**, **3Q** and **4Q**, respectively. The binding ratio of **2Q**, **3Q** and **4Q** to DNA is 0.61 ± 0.8 , 0.52 ± 0.7 and 0.56 ± 0.8 , respectively.

These results were consistent with UV-Vis titrations indicating a non-intercalative but minor groove binding with DNA.

3.4. Determination of quenching effect of **2Q**, **3Q** and **4Q** on the fluorescence intensity of DNA-SYBR complex by using K_{sv} constants

SYBR Gold is a known DNA stain used in biological applications [44]. In solution, the unbound SYBR exhibits very little fluores-

cence, however, a greatly enhanced fluorescence upon DNA-binding is observed at 540 nm [44]. When compared with the other minor groove binders like DAPI (4,6-diamino-isophenylindole) and Hoescht, SYBR is not sensitive to double or single strand DNA and the structure is more stable in acidic or basic media [44]. Therefore, a competition of binding assay between SYBR and novel quaternized pcs **2Q**, **3Q** and **4Q** would demonstrate the mode of interaction with DNA. This assay was easy to detect, as fluorescence of free SYBR-DNA complex was notably diminished by the strong fluorescence quenching effects of quaternized compounds. The quenching effect was determined by using K_{sv} constants (Table 1). The K_{sv} value of **2Q** was higher than **3Q** and **4Q** indicating that the smaller the cationic group [45] the more binding affinity to DNA and the more quenching effect on fluorescence of SYBR-DNA complex is. The quenching process depends on the formation of a stable pc-DNA complex less fluorescent than free pc. The more the stable pc-DNA complex formed, the less the fluorescence was observed. This means that DNA preferred pc instead of SYBR. Thus the decrease in fluorescence emission evidenced the existence of an effective interaction between pcs and DNA. These results were in agreement with K_a values supporting an electrostatic external binding to DNA phosphates (Table 1, Fig. 5).

3.5. Determination of the change in thermal denaturation profile of DNA

The DNA thermal melting is a measure of the stability of the DNA double helix with temperature; an increase in the thermal melting temperature (T_m) indicates an interaction between DNA and the metal complex. In the present case, T_m values were deter-

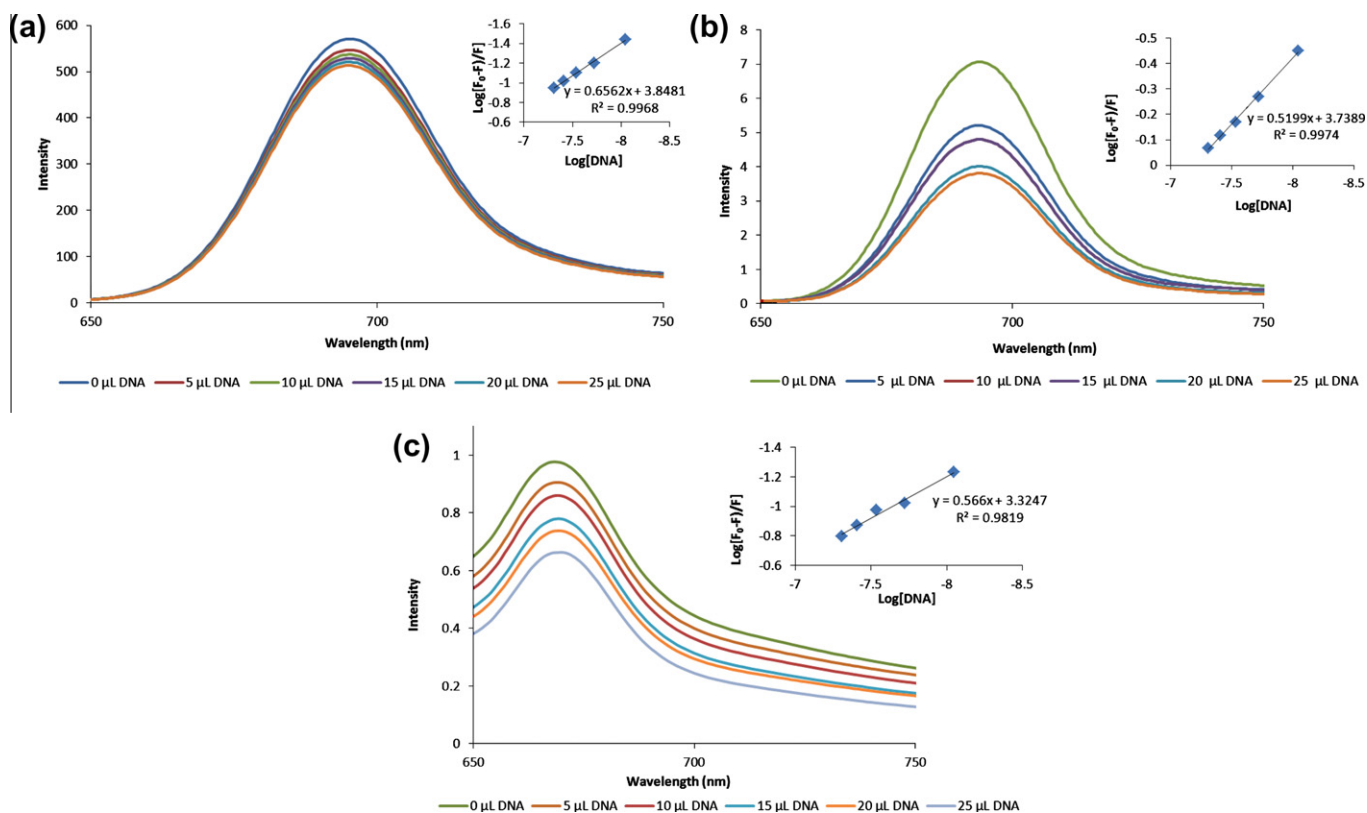


Fig. 4. Fluorescence emission spectral changes of **2Q** (a) **3Q** (b) and **4Q** (c) on addition of varying concentrations of DNA in water. Insets: The plot for determination of binding constants of **2Q** (a), **3Q** (b) and **4Q** (c) to DNA. All samples were excited at 610 nm.

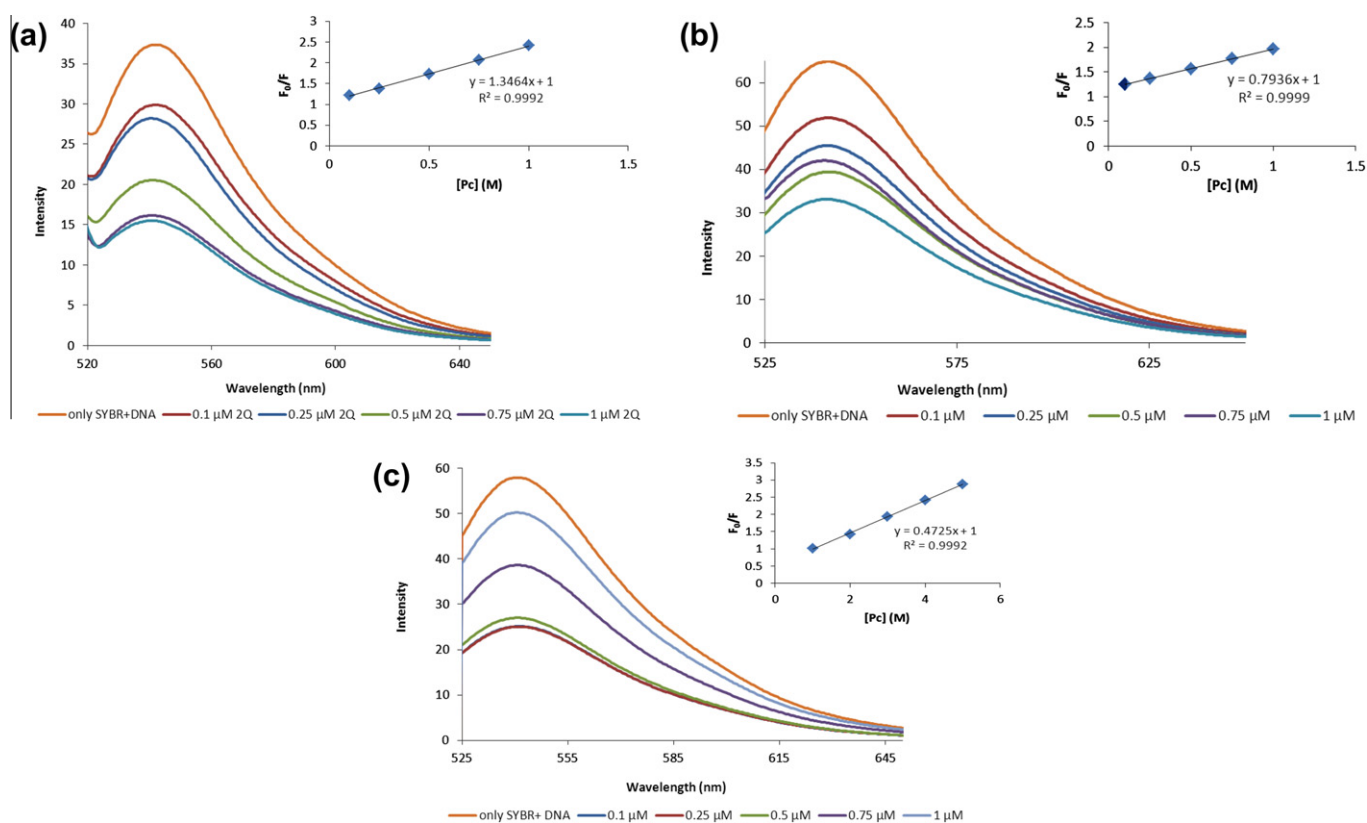


Fig. 5. (a) The fluorescence emission spectral changes of SYBR–DNA complex (1×10^{-5} M SYBR and 5 μM , 1.8 mL DNA) upon the additions of varying concentrations of **2Q** (a), **3Q** (b) or **4Q** (c). Insets: The plot drawn to determinate K_{SV} quenching constant of **2Q** (a), **3Q** (b) and **4Q** (c) on the fluorescence of SYBR–DNA complex. All samples were excited at 497 nm.

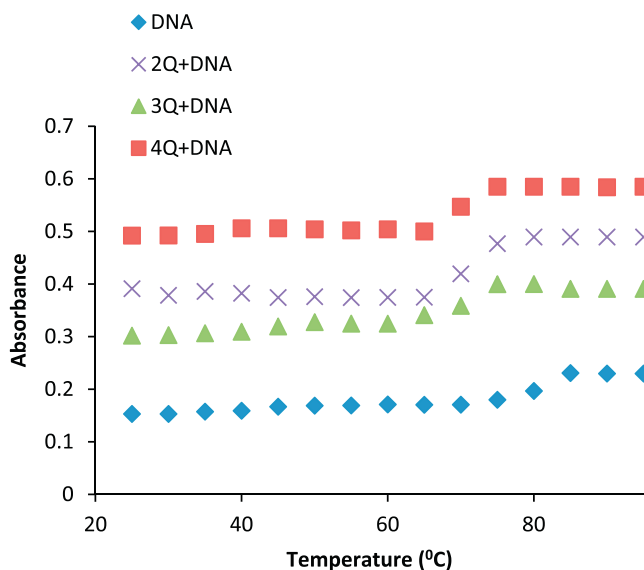


Fig. 6. The thermal denaturation profiles of DNA in the absence and presence of **2Q**, **3Q** and **4Q**.

mined by monitoring the absorbance of DNA at 260 nm as a function of temperature. T_m of DNA in the absence of any added drug was found to be $80\text{ }^\circ\text{C} \pm 0.2$, under our experimental conditions. Under the same set of conditions, the presence of complexes **2Q**, **3Q** and **4Q** decreased ΔT_m by 2.5, 2.5 and 5 $^\circ\text{C}$ respectively. The melting temperature of DNA (T_m) in the presence of a binding molecule can also be used to distinguish between intercalative and external binding modes. Usually, classical intercalation gives rise to higher ΔT_m values than either groove binding or outside stacking [31]. The thermal denaturation results for the binding of **2Q–4Q** to CT-DNA are shown qualitatively in Fig. 6. As known, the absorption of double strand DNA is lower than the single strand DNA and high pH values decrease T_m [46]. According to our experimental results, quaternized amines especially in compound **4Q** increased pH of the working solutions and denatured double strand DNA resulting the formation of single strand DNA due to scissoring at a lower temperature (decreased T_m 5 $^\circ\text{C}$) than **2Q** and **3Q** did (decreased T_m 2.5 $^\circ\text{C}$). These results were consistent with the determined K_a values further stressing an external binding took place between DNA and pcs.

3.6. Determination of binding **2Q**, **3Q** and **4Q** to DNA using gel electrophoresis

The binding of quaternized pcs **2Q–4Q** was examined with gel electrophoresis. 1% agarose gel was prepared and TBE buffer was used for staining solution. The migration of a series of dye/DNA complexes of different ratios (Table 2) are shown in Fig. 7. It was important to see whether DNA would prefer pcs or SYBR to bind. Thus, the gels were stained by SYBR upon electrophoretic run. It was observed that at low ratios of pcs to DNA, an excess of uncomplexed DNA was present as shown by the migration of the DNA bands. The migration of DNA in the gel was regarded as the ratio of dye to DNA increased, indicating that pcs were capable of binding to DNA, neutralizing its charges. Fig. 7 indicated that **2Q** had affinity to bind DNA and complete neutralization occurred between phosphates and quaternized amines of **2Q** at an R value of 1.5. In case of **3Q**, there was no complete neutralization between positive and negative charges even at high R values such as 1.5 and 2. This was the evidence for hindrance of the interaction between DNA and bigger hydrophilic groups. Fig. 7 showed that there was still uncomplexed DNA (in presence of **3Q**) and migration at

Table 2

Explanation for R values in gel electrophoresis (agarose 1%) in Fig. 7, indicating the interaction of **2Q**, **3Q** and **4Q** with DNA.

R	[2Q]/[DNA]	[3Q]/[DNA]	[4Q]/[DNA]
0	^a M	M	M
0.25 (1.25 $\mu\text{L}/5\text{ } \mu\text{L}$)	1	6	11
0.5 (2.5 $\mu\text{L}/5\text{ } \mu\text{L}$)	2	7	12
1 (5 $\mu\text{L}/5\text{ } \mu\text{L}$)	3	8	13
1.5 (7.5 $\mu\text{L}/5\text{ } \mu\text{L}$)	4	9	14
2.0 (10 $\mu\text{L}/5\text{ } \mu\text{L}$)	5	10	15

^a M is DNA marker to note the direction of migration.

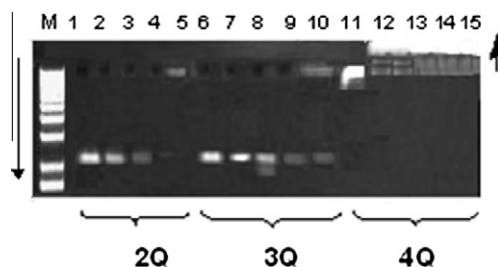


Fig. 7. The gel electrophoresis pattern of DNA in the presence of **2Q**, **3Q** and **4Q**. R values were given in Table 2. M is DNA marker to note the direction of migration.

the highest R value was also observed. When the more neutralization occurred, the less migration on the gel was seen. However, more positive charge caused opposite migration which was seen for compound **4Q**. At low R value there was almost complete neutralization and as seen in Fig. 7, quaternized **4Q** was stuck in the well together with DNA at the top of the gel. However, at a higher R value caused a migration at opposite direction. This was due to high positive charge of **4Q**. According to Fig. 7, gel electrophoresis pattern indicated that the cationic unit of pcs is neutralizing the negative charges of DNA, thereby resulting the formation of a stable complex in case of **2Q** and **3Q** at high R values (charges on **2Q**, **3Q** and **4Q** are 2+, 2+ and 6+, respectively) while **4Q** does at low R values because of its charge.

3.7. Determination of photocleavage of plasmid DNA using gel electrophoresis

Since the novel pcs presented here demonstrated DNA binding property, the efficient use of these materials in PDT would be the photocleavage of DNA. Thus, to observe this phenomenon, supercoiled DNA was used and it was irradiated with a diode laser in the presence of **2Q**, **3Q** and **4Q**. The characteristic photodegradation of ADMA at 380 nm was observed when the solutions that contain ADMA together with quaternized pcs were irradiated by a diode laser (Fig. 8).

No DNA scission was observed when the photosensitizer was kept in the dark even though **2Q**, **3Q** and **4Q** were present. Moreover, to prove the involvement of singlet oxygen in photocleavage, we used sodium azide as singlet oxygen trap. In the absence of sodium azide, nicked form was observed, opposing to the presence of singlet oxygen trap (Fig. 8: Lanes 7). When plasmid DNA was subjected to electrophoresis, fast migration was observed for the supercoiled (form I). If scission occurred on one strand (nicking), the supercoils would relax to generate a slower-moving open circular form (form II). A concentration-dependent DNA scission was experienced for all quaternized pcs and the binding of pcs were tested without irradiation at different concentrations (Fig. 7). Thus, the effect of irradiation was evaluated at a constant concentration of reactants with changing irradiation time. As shown in Fig. 8, longer time of irradiation exhibited greater photodamage and

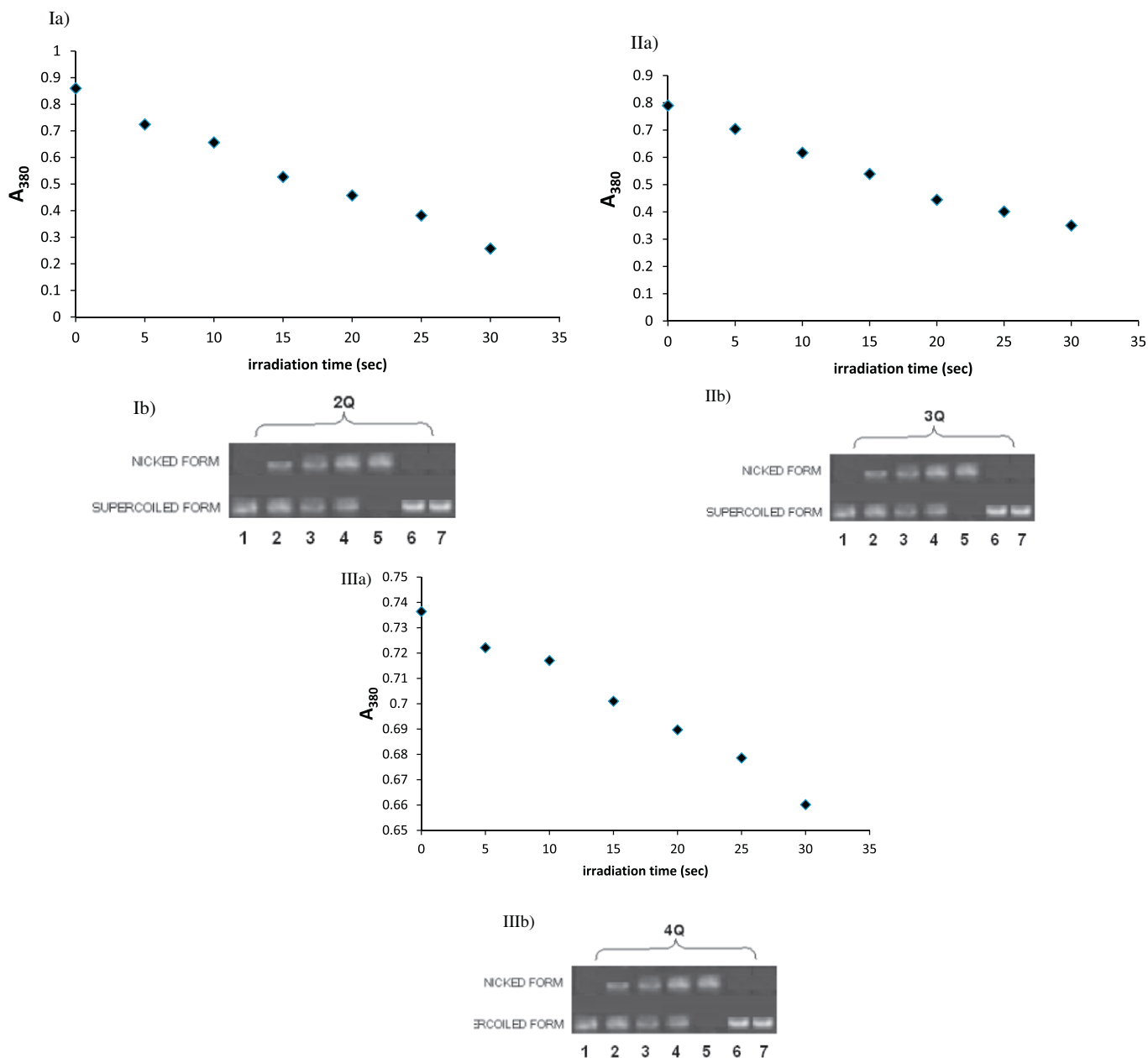


Fig. 8. The decreases in absorbance of ADMA at 380 nm in the presence of **2Q** (Ia), **3Q** (IIa) and **4Q** (IIIa) due to singlet oxygen generation. Agarose (1%) gel electrophoresis pattern for the photocleavage of pBR322 by **2Q** (Ib), **3Q** (IIb) and **4Q** (IIIb). Reaction mixtures contained 10 μ L (0.2 μ g) pBR322. Lanes 1: pBR322 only. Lanes 2: **2Q** (Ib), **3Q** (IIb) and **4Q** (IIIb) + pBR322 + 1 min irradiation. Lanes 3: **2Q** (Ib), **3Q** (IIb) and **4Q** (IIIb) + pBR322 + 3 min irradiation. Lanes 4: **2Q** (Ib), **3Q** (IIb) and **4Q** (IIIb) + pBR322 + 5 min irradiation. Lanes 5: pBR322 + **2Q** (Ib), **3Q** (IIb) and **4Q** (IIIb). Lanes 6: pBR322 + 5 min irradiation ($\lambda > 650$). Lanes 7: **2Q** (Ib), **3Q** (IIb) and **4Q** (IIIb) + pBR322 + 0.2 M sodium azide + 5 min irradiation.

formed nicked form DNA. (Lanes 2–4 in Fig. 8: Ib, IIb and IIIb for **2Q**, **3Q** and **4Q** respectively). The binding of pcs to supercoiled DNA was proved with control groups without irradiation (Lanes 5 in Fig. 8: Ib, IIb and IIIb). There was no effect of irradiation on supercoiled DNA (Lanes 6 in Fig. 8: Ib, IIb, and IIIb). Therefore, these water soluble pcs have the ability for DNA scission.

4. Conclusion

In the present work, both neutral and water soluble silicon pcs were successfully accomplished. As known, cationic moieties can bind to DNA either intercalatively or electrostatically [31,41] and

water soluble nature of drugs enhances the cellular uptake for PDT. Thus, taking into consideration PDT activity, pcs which are incorporated with silicon were chosen to be examined.

The binding of all three quaternized compounds **2Q–4Q** to DNA was determined by using K_a binding constants, agarose gel electrophoresis, Stern Volmer quenching constants and thermal profiles of DNA. According to our results, new quaternized pcs have the affinity to bind to external phosphates of DNA backbone. Besides, singlet oxygen generation of **2Q**, **3Q** and **4Q** (Fig. 8: Ia, IIa and IIIa) was proved in aqueous media by the photodegradation of ADMA. The combination of two different experiments; the binding affinity of **2Q–4Q** to DNA and singlet oxygen generation provided to demonstrate the photocleavage of pBR322 via irradiation in the pres-

ence of **2Q**, **3Q** or **4Q** (Fig 8: Ib, IIb and IIIb). Thus, novel water soluble silicon pcs might be the candidates for PDT or other biological applications. The ongoing research on the response of these dyes in organelles of yeasts is worthwhile.

Acknowledgment

This work was supported by TUBITAK (110T527) and Research Fund of Istanbul Technical University.

References

- [1] S. Riahi, S. Eynollahi, M.R. Ganjali, *Chem. Biol. Drug Des.* 76 (2010) 425.
- [2] G. Bischoff, S. Hoffmann, *Curr. Med. Chem.* 9 (2002) 321.
- [3] M. Wainwright, *Biotech. Histochem.* 85 (2010) 341.
- [4] C.C. Leznoff, A.B.P. Lever, *Phthalocyanines: Properties and Applications*, vol. 1, VCH, New York, 1989.
- [5] N.B. McKeown, Cambridge University Press, 1998.
- [6] K. Kadish, K.M. Smith, R. Guilard, *The Porphyrin Handbook*, vol. 15–20, Academic Press, Boston, 2003.
- [7] R. Haimovici, T.A. Ciulla, J.W. Miller, T. Hasan, T.J. Flotte, A.G. Kenney, *Retina* 22 (2002) 65.
- [8] M. Eldar, Y. Yerushalmi, E. Kessler, M. Scheinowitz, U. Goldbourt, E. Ben-Hur, V. Rosenthal, *A. Battler, Atherosclerosis* 84 (1990) 135.
- [9] C. Monica, M. Michela, S. Marina, G. Jori, M. Moreno, I. Chambarier, M.J. Cook, D.A. Russell, *Eur. J. Cancer* 46 (2010) 1910.
- [10] P.C. Lo, C.M.H. Chan, J.Y. Liu, W.P. Fong, D.K.P. Ng, *J. Med. Chem.* 50 (2007) 2100.
- [11] M. Çamur, V. Ahsen, M. Durmuş, *J. Photochem. Photobiol. A* 219 (2011) 217.
- [12] F. Dumoulin, M. Durmus, V. Ahsen, T. Nyokong, *Chem. Rev.* 254 (2010) 2792.
- [13] M. Durmuş, V. Ahsen, *J. Inorg. Biochem.* 104 (2010) 297.
- [14] E. Ben-Hur, I. Rosenthal, *Int. J. Radiat. Biol.* 47 (1985) 145.
- [15] R.L. Morris, A. Kashif, M. Lam, J. Berlin, A.L. Nieminen, M.E. Kenney, A.C.S. Samia, C. Burda, N.L. Oleinick, *Cancer Res.* 63 (2003) 5194.
- [16] N.L. Oleinick, A.R. Antunez, M.E. Clay, B.D. Rihter, M.E. Kenney, *Photochem. Photobiol.* 57 (1993) 242.
- [17] S.I.A. Zaidi, R. Agarwal, G. Eichler, B.D. Rihter, M.E. Kenney, H. Mukhtar, *Photochem. Photobiol.* 58 (1993) 204.
- [18] R.L. Morris, M.E. Varnes, M.E. Kenney, Y.S. Li, N.L. Oleinick, *Photochem. Photobiol.* 75 (2002) 652.
- [19] L.Y. Xue, N.L. Oleinick, *Oncogene* 24 (2005) 6987.
- [20] D.V. Sakharov, W.E. Hennink, C.F. Nostrum, *J. Med. Chem.* 50 (2007) 1485.
- [21] E. Ben-Hur, J. Oetjen, B. Horowitz, *Photochem. Photobiol.* 65 (1997) 456.
- [22] J. Mao, Y. Zhang, J. Zhu, C. Zhang, Z. Guo, *Chem. Commun.* (2009) 908.
- [23] A. Vogge, E. Lork, B.Ş. Sesalan, D. Gabel, *J. Organomet. Chem.* 694 (2009) 1698.
- [24] B.Ş. Sesalan, A. Koca, A. Gül, *Polyhedron* 22 (2003) 3083.
- [25] B.Ş. Sesalan, A. Koca, A. Gül, *Chemie* 131 (2000) 1191.
- [26] B.Ş. Sesalan, A. Gül, *Phosphorus Sulfur* 178 (2003) 2081.
- [27] B.Ş. Sesalan, A. Koca, A. Gül, *Dyes Pigm.* 79 (2008) 259.
- [28] M.K. Gümüştaş, B.Ş. Sesalan, P. Atukeren, B. Yılmaz, A. Gül, *J. Coord. Chem.* 63 (2010) 4319.
- [29] B. Turanlı-Yıldız, T. Sezgin, Z.P. Çakar, C. Uslan, B.Ş. Sesalan, A. Gül, *Synth. Met.* 161 (2011) 1720.
- [30] C. Uslan, B.Ş. Sesalan, *Dyes Pigm.* 94 (2012) 127.
- [31] W. Duan, W. Zhenxin, M.J. Cook, *J. Porphyrins Phthalocyanines* 13 (2009) 1255.
- [32] X.Z. Feng, Z. Lin, L.J. Yang, C. Wang, C. Bai, *Talanta* 47 (1998) 1223.
- [33] E. Safaei, B. Ranjbar, L. Hasani, *J. Porphyrins Phthalocyanines* 11 (2007) 805.
- [34] J.H. Brannon, D.J. Madge, *Am. Chem. Soc.* 102 (1980) 62.
- [35] I. Seotsanyana-Mokhosi, N. Kuznetsova, T. Nyokong, *J. Photochem. Photobiol. A* 140 (2001) 215.
- [36] W. Spiller, H. Kliesch, D. Wöhrle, S. Hackbarth, B. Roder, G. Schnurpfeil, *J. Porphyrins Phthalocyanines* 2 (1998) 145.
- [37] X.J. Jiang, P.C. Lo, Y.M. Tsang, S.L. Yeung, W.P. Fong, D.K.P. Ng, *Chem. Eur. J.* 16 (2010) 4777.
- [38] H. Li, T.J. Jensen, F.R. Fronczek, M.G.H. Vicente, *J. Med. Chem.* 51 (2008) 502.
- [39] X.J. Jiang, J.D. Huang, Y.J. Zhu, F.X. Tang, D.K.P. Ng, J.C. Sun, *Bioorg. Med. Chem. Lett.* 16 (2006) 2450.
- [40] M.E. Anderson, A.G.M. Barrett, B.M. Hoffman, *J. Inorg. Biochem.* 80 (2000) 257.
- [41] A.M. Zhanga, J. Huang, X. Wenga, J.X. Lia, L.G. Rena, Z. Songa, X. Xionga, X. Zhou, X. Caod, Y. Zhoue, *Chem. Biodivers.* 4 (2007) 215.
- [42] M.J. Lee, B. Jin, H.M. Lee, M.J. Jung, S.K. Kim, J.M. Kim, *Bull. Korean Chem. Soc.* 29 (2008) 1533.
- [43] M. Monajjemi, H. Aghaie, F. Naderi, *Biochemistry (Moscow)* 72 (2007) 652.
- [44] G. Cosa, K.S. Focsaneanu, J.R.N. McLean, J.P. McNamee, J.C. Scaiano, *Photochem. Photobiol.* 73 (2001) 585.
- [45] V. Jadhav, S. Maiti, *Biomacromolecules* 9 (2008) 1852.
- [46] K.R. Fox, *Drug-DNA Interaction Protocols*, vol. 90, Humana Press, New Jersey, 1997.